Journal of Proteomics 142 (2016) 33–44

Contents lists available at ScienceDirect

Journal of Proteomics

journal homepage: www.elsevier.com/locate/jprot

Monitoring light/dark association dynamics of multi-protein complexes in cyanobacteria using size exclusion chromatography-based proteomics

Ana C.L. Guerreiro [a,b], Renske Penning [a,b], Linsey M. Raaijmakers [a,b], Ilka M. Axman [c], Albert J.R. Heck [a,b,*], A.F. Maarten Altelaar [a,b,*]

[a] Biomolecular Mass Spectrometry and Proteomics, Utrecht Institute for Pharmaceutical Sciences and Bijvoet Centre for Biomolecular Research, Utrecht University, Padualaan 8, 3584 CH Utrecht, The Netherlands
[b] Netherlands Proteomics Centre, Padualaan 8, 3584 CH Utrecht, The Netherlands
[c] Institute for Synthetic Microbiology, Heinrich Heine University Duesseldorf, Universitaetsstrasse 1, D-40225 Duesseldorf, Germany

ARTICLE INFO

Article history:
Received 18 September 2015
Received in revised form 11 March 2016
Accepted 19 April 2016
Available online 29 April 2016

ABSTRACT

Diurnal rhythms are recurring 24 h patterns such as light/dark cycles that affect many natural environmental and biological processes. The cyanobacterium *Synechococcus elongatus* PCC 7942 (*S. elongatus*) produces its energy through photosynthesis and therefore its internal molecular machinery is strongly influenced by these diurnal rhythms. Moreover, it has one of the simplest, self-sustained, circadian rhythms, extensively studied functionally and structurally. These characteristics together with the relatively small genome of *S. elongatus*, make it an ideal model system for the study of diurnal and circadian rhythms. Although expression of many gene transcripts has been shown to fluctuate in phase with the circadian rhythm, fluctuations at the protein level were less pronounced. This led us to hypothesize that the diurnal adaptation occurs at the level of higher organization of protein complexes. Therefore, we probed the abundance and constituency of *S. elongatus* protein complexes during the day and night. Following several well-known complexes such as the RNA polymerase, the ribosome and photosynthetic protein complexes, we observe for the first time that these complexes change not only in abundance but also in constituency. Therefore, we conclude that the dynamic assembly of protein complexes is indeed also a key-player in the processes governing the diurnal rhythm.

Significance: The succession of day and night periods imposes drastic changes in all living organisms. Cyanobacteria produce their energy through photosynthesis and are therefore strongly influenced by diurnal rhythms. The cyanobacteria, *Synechococcus elongatus* PCC 7942 (*S. elongatus*), also exhibit a self-sustained biological clock. The connection between the central circadian oscillator and its output to the rest of the cell is not completely known. It has been shown that the expression of many gene transcripts heavily fluctuates in phase with the circadian rhythm; however, our recent global proteomics investigation revealed that the diurnal fluctuations seemed to be less pronounced at the protein level. As many known regulatory functions depend on protein-protein interactions (PPIs) and/or protein assemblies and the fact that so few fluctuations in protein abundances were observed earlier, here we investigated the diurnal adaptation at the level of dynamic changes in protein assembly.

The paper demonstrates that the combination of native protein complex fractionation and high-resolution proteomics provides insight in the regulation of megadalton protein assemblies in cyanobacteria, including the ribosomal and photosynthetic complexes. The differences observed between the light and dark conditions in these complexes indicate a cyclic regulation of essential cellular processes.

1. Introduction

The succession of day and night periods imposes drastic changes in all living organisms, during which also different molecular processes adapt. These may include different regulatory mechanisms and cellular pathways, such as the photosynthetic pathway, which occurs primarily during the day when sunlight is available. These different processes are usually entrained with the day and night cycles either through diurnal rhythms or through so-called circadian rhythms. Diurnal rhythms are biological cycles dependent on external cues, such as light and dark variations. On the other hand, circadian rhythms are adjustable to those cues, but they are also self-sustained biological cycles of 24 h. Both types of rhythms are widely present in all kingdoms of life, including

* Corresponding authors at: Biomolecular Mass Spectrometry and Proteomics, Utrecht Institute for Pharmaceutical Sciences and Bijvoet Centre for Biomolecular Research, Utrecht University, Padualaan 8, 3584 CH Utrecht, The Netherlands.
E-mail addresses: a.j.r.heck@uu.nl (A.J.R. Heck), m.altelaar@uu.nl (A.F.M. Altelaar).

http://dx.doi.org/10.1016/j.jprot.2016.04.030
1874-3919/

in lower complexity organisms such as cyanobacteria [1]. The circadian rhythms in particular, have non-universal molecular mechanisms governing them, differing from species to species, and they are known to be rather complex, involving many genes in higher eukaryotic systems. Cyanobacteria, such as the *Synechococcus elongatus* PCC 7942 (*S. elongatus*), also exhibit a self-sustained biological clock, which is from a molecular perspective much more simple. Therefore, the cyanobacterial model, with its rather small genome (2.7 Mbp) [2,3], has been widely adopted to investigate circadian regulation [2,4–6]. The central core of this very robust pacemaker is composed of only three proteins, namely KaiA, KaiB and KaiC. In short, the mechanism involves the cyclic phosphorylation/dephosphorylation of KaiC, by KaiA or KaiB, respectively, which also dynamically regulates the assembly of these three proteins into larger protein complexes [6,7].

The connection between the central circadian oscillator and its output to the rest of the cell is not completely known. Although it has been shown that the expression of many gene transcripts heavily fluctuates in phase with the circadian rhythm [5,8], our recent global proteomics investigation revealed that the diurnal fluctuations seemed to be less pronounced at the protein level [4]. It has been established that the central clock regulates gene expression through several effectors, such as the histidine kinase SasA (*Synechococcus* adaptive sensor), the master regulator RpaA (regulator of phycobilisome-associated A/two component transcriptional regulator) [9–11], the RpaB regulator [12], LabA (low amplitude and bright A) and the sensor histidine kinase CikA (circadian input kinase A) [13,14]. The central clock is in turn entrained by the input factors Pex (PadR family transcriptional regulator) and LdpA (light-dependent period A). The regulatory functions mentioned above, and many others, depend on protein-protein interactions (PPIs) [15] and/or protein assemblies. Taking this into account and the fact that so few fluctuations in protein abundances were observed earlier [4], we argued that the diurnal adaptation might occur at the level of dynamic changes in protein assembly. Therefore, here we set out to analyze the relative abundance and constituencies of protein assemblies in cyanobacteria at the maximum of the light and dark phases.

The most common approaches for the study of protein interactions and assemblies consist of either yeast two-hybrid screens [16] or affinity purification coupled to mass-spectrometry (AP-MS) [17,18]. In the latter, the protein of interest is used as a “bait” to isolate and “pull down” its interacting proteins. AP-MS has been widely used and nowadays allows the comparison of different complexes at the same time [19,20], with increasingly high-throughput [21,22]. It has been applied for instance to map full interactomes, also in the bacteria *Escherichia coli* [23]. As a minor drawback of the approach, it has been shown that this technique, by using N- or C-terminal tags, can affect protein interactions and functions [24,25], besides being limited by the availability of tagged-constructs or antibodies, restraining the study of the dynamic PPIs across many conditions. Ultimately, as a targeted approach, AP-MS can only identify complexes of baits chosen *a priori*, disregarding the dynamics of unexpected PPIs. Recently, an alternative method was introduced coupling size exclusion chromatography (SEC) and high-resolution MS, which tackles some of the disadvantages of AP-MS. SEC is a widely used classical biochemistry technique in which proteins in solution are separated according to their shape/size. Under native conditions, this technique can be used to separate protein oligomers and or complexes based on their size and can be used as a pre-fractionation step prior to mass spectrometry based proteomics analysis. This strategy has already been applied to chloroplast samples [26], as well as human cell lysates [27,28].

To our knowledge, a global analysis of the PPIs of *Synechococcus elongatus* has not yet been performed, and there is even more limited information on how such complexes would adapt to day (light) and night (dark) conditions. *A priori* it may be hypothesized that biological processes such as photosynthesis, which is regulated by large protein assemblies, display night and day differences, possibly reflected by the recruitment or disassembly of different accessory proteins. Similarly, essential cellular processes, such as transcription and protein synthesis, previously associated with circadian regulation, may display differences. To study adaptation of the *S. elongatus* PPIs' to light and dark conditions, we used an MS centered approach conjugated with the pre-fractionation of protein assemblies by SEC. To compare the light and dark (LD) variations in protein complexes, we used *S. elongatus* cultures grown in LD cycles (12:12 h) and collected samples from two opposite time-points separated by 12 h: one from the light phase and one from the dark phase. The protein complexes obtained were separated according to their size by SEC, and identified and quantified through a high-resolution MS data was obtained using/MS approach, using standard protein complexes as internal standards. Using biological duplicates we were able to identify protein complexes from 100 kDa up to several megadalton (MDa), and analyze differences in their composure under light and dark conditions. Our data on several different protein assemblies include confirmations of previous observations, but also provides evidence for the putative role of new protein constituents in playing specific roles at either the night or day phase of the cyanobacteria.

2. Methods

2.1. Cyanobacteria cell culture

The wild-type strain of *Synechococcus elongatus PCC 7942* was grown as previously described [29] photoautotrophically in BG11-medium at 30 °C under continuous illumination with white light of 80 μmol of photons/m^2 s (Versatile Environmental Test Chamber, SANYO) and a continuous stream of air. Cell concentrations were measured by determining the optical densities of the culture at 750 nm (OD750) (SPECORD®200 PLUS, Analytik Jena). The culture was kept in log growth phase (up to an OD750 of 1.0) by dilution up to a specific volume and transferred to 12:12-hour light/dark cycle (LD) for 3 days. Synchronized culture was finally diluted to an OD750 of approximately 0.4 1 day before the sampling started. Two time points with 12 h intervals were sampled, for each of the two replicates. 40 ml of the culture was centrifuged at 15,000*g* for 10 min and the supernatant was removed. Cell pellet was resuspended in 1 ml BG11-medium, centrifuged again for 5 min. Supernatant was removed and pellet washed with 1 ml PBS buffer before last round of centrifugation. Cell pellets were frozen in liquid nitrogen prior to storage at −20 °C.

2.2. Cell lysis

Cyanobacteria pellets were lysed in 50 mM KCl, 50 mM NaCOO (pH = 7.2), containing 1 tablet EDTA-free protease inhibitor cocktail (Sigma) and 1 tablet PhosSTOP phosphatase inhibitor cocktail (Roche). After three mild sonication cycles at 4 °C, total cell lysates were obtained through centrifugation at 14,000 rpm for 20 min, at 4 °C. The supernatant was recovered and protein concentrations were determined with the Bradford method (BioRad). A Vivaspin500 100kMWCO filter (Sartorius Stedim Biotech GmbH, Goettingen, DE) was used to pre-select protein complexes larger than 100 kDa, by centrifugation at 15,000 RCF at 4 °C.

2.3. SEC (size-exclusion chromatography)

The filtered cyanobacterial cell lysates were mixed with a mixture of protein and protein complex standards (Sigma-Alderich, St Louis, US), containing: thyroglobulin (3.3 μM, 669 kDa, complex), apoferritin (3.1 μM, 443 kDa, complex), beta-amylase (5.5 μM, 200 kDa, complex), alcohol dehydrogenase (9.1 μM, 150 kDa, complex) and carbonic anhydrase (28 μM, 29 kDa). For SEC the samples were injected (100 μl) onto a BioSep SEC S4000 column (Phenomenex) with a fractionation range of 15–1500 kDa, supported by an Akta Basic HPLC system (GE Healthcare). Equilibration and elution were performed with

50 mM KCl, 50 mM NaCOO (pH = 7.2). The flow rate was 450 μl/min and 54 fractions were collected at 260 μl/min, into Eppendorf tubes.

2.4. In solution digestion

The protein complexes collected in the SEC fractions were denatured using Rapigest (Waters) surfactant and subjected to 99 °C incubation for 5 min. Next, reduction and alkylation of the cysteine residues was performed using 200 mM dithiotreitol (DTT) (Sigma) and 200 mM iodoacetamide (Sigma), respectively. The proteins were first digested with Lys-C (Roche Diagnostics, Ingelheim, Germany), at an enzyme:protein ratio of 1:75, for 4 h at 37 °C, followed by digestion with trypsin (Roche Diagnostics, Ingelheim, Germany), at an enzyme:protein ratio of 1:100, overnight at 37 °C. Samples were desalted using an Oasis μElution plate (Waters) and dried *in vacuo*. The bovine serum albumin (Sigma) spiked-in later and used for normalization was digested separately, under similar conditions, with the exception of the surfactant being substituted by a solution of 8 M urea and 50 mM ammonium bicarbonate.

2.5. Liquid chromatography-tandem mass spectrometry (LC-MS/MS)

LC-MS/MS data was obtained using a Q Exactive Orbitrap (Thermo Fisher Scientific, Bremen) that was coupled to an Agilent 1290 Infinity UHPLC (Ultra-High Pressure Liquid Chromatography) system (Agilent Technologies, Waldbronn, DE). Both the trap (20 mm × 100 μm i.d.) and the analytical column (35 cm × 50 μm i.d.) were packed in-house using Poroshell C18 2.7 μm (Agilent Technologies, Waldbronn, DE). Peptides were trapped at 5 μl/min in 100% solvent A (0.1 M acetic acid (Merck)). Elution was achieved with the solvent B (0.1 M acetic acid in 80% acetonitrile) at 100 nl/min. The 60 min gradient used was as follows: 0–10 min, 100% solvent A; 10.1–45 min, 13–41% solvent B; 45–48 min, 41–100% solvent B; 48–49 min, 100% solvent B; 49–50 min, 0–100% solvent A; 50–60 min, 100% solvent A. The autosampler was programed to inject 2 fmol of tryptic digest of bovine serum albumin prior to sample injection. Nanospray was achieved using a coated fused silica emitter (New Objective, Cambridge, MA) (o.d. 360 μm; i.d. 20 μm, tip i.d. 10 μm) biased to 1.7 kV. The mass spectrometer was operated in the data dependent acquisition mode. A MS2 method was used with a FT survey scan from 350 to 1500 *m/z* (resolution 35,000; AGC target 3E6). The 10 most intense peaks were subjected to HCD fragmentation (resolution 17,500; AGC target 5E4, NCE 25%, max. injection time 120 ms, dynamic exclusion 10 s). Predictive AGC was enabled.

2.6. Database search and validation

Raw data was analyzed by using Proteome Discoverer (version 1.3, Thermo), with the Mascot search engine (version 2.3.02, Matrix science). MS/MS data was searched against the *S. elongatus* PCC 7942 Uniprot database (version 4-2010) including a list of common contaminants and concatenated with the reversed versions of all sequences (5826 sequences). The sequences from the SEC standard proteins and protein complexes (alcohol dehydrogenase, beta-amylase, apo-ferritin, carbonic anhydrase and thyroglobulin) and the bovine serum albumin were also added to this database. Trypsin was chosen as cleavage specificity allowing two missed cleavages. Carbamidomethylation (C) was set as a fixed modification. The variable modification used was methionine oxidation. The database searches were performed considering all charge states, using a peptide tolerance of 50 ppm and a fragment mass tolerance of 0.05 Da (HCD). The 50-ppm mass window was chosen to allow random assignment of false positives that were later removed by filtering using the instruments actual mass accuracy (10 ppm). The peak area of each protein was obtained using the Precursor ion area detector node in Proteome discoverer. Here, the protein peak area is calculated by an average of the 3 most intense distinct peptides, i. e. with distinct sequences [30]. After performing the independent searches of all SEC fractions, these results were combined for visualization, using identifications thresholds of a minimum peptide score of 20, a peptide rank of 1, a peptide length between 6 and 23 amino acids and a high peptide confidence. Finally, the peak area data was exported from Proteome discoverer for further processing.

2.7. Data processing and analysis

The peak area of the spiked-in BSA internal standard was used for normalization. Each fraction was normalized according to the average peak area of BSA, calculated across all fractions. This was followed by a similar normalization per experiment. The peak areas from the two biological replicate experiments were averaged. The proteins identified with less than two peptides, consequently with lower confidence, were excluded. Finally, since the SEC standard proteins were added with the same quantity to each replicate, we also normalized the peak areas to give a standard constant peak area ratio of 1 for the protein standards between light and dark.

To identify protein complexes that display regulated features between the night and day phase, we compared the averaged profiles of light and dark using an in-house developed analysis and visualization tool. Perseus software (http://www.perseus-framework.org/) was used for the clustering analysis and replicate correlation calculations. For all the hierarchical clustering analysis made, we first performed a Z-score normalization on the peak areas from light and dark, simultaneously, this allows better correlation of protein profiles, although one can only compare abundances between light and dark conditions. Secondly, we performed an imputation of the missing values by substituting them with zero; finally, we performed the unsupervised clustering of the rows using Pearson correlation, with k-means pre-processing and a complete linkage. The approximate molecular weight corresponding to each fraction was calculated considering the theoretical molecular weight of the SEC standard proteins and protein complexes and their elution profiles. A logarithmic function was fitted to this distribution to extrapolate the molecular weight across all fractions.

3. Results and discussion

In many organisms, biological processes such as transcription, translation and photosynthesis follow circadian patterns and are regulated by large proteins assemblies. Cyanobacteria represent some of the oldest organisms that exhibit a very simple but effective circadian rhythm. Here, we set out to provide a global quantitative label-free analysis of native protein complexes originating from the cyanobacteria *Synechococcus elongatus* PCC7942, under light and dark (LD) conditions, using a combination of size exclusion chromatography (SEC) and high-resolution mass spectrometry (LC-MS/MS) (Fig. 1A). To evaluate LD variations in protein complexes, we selected two “extreme” time-points separated by 12 h across a 24-h LD cycle, specifically one in the middle of the light phase and one in the middle of the dark phase. By using mild cell lysis conditions, we were able to preserve protein complexes in their native state and subsequently separate them according to their complex/protein size, using SEC. The SEC chromatograms obtained were reproducible between light and dark samples and corresponding biological replicates, as shown by their overlap (Fig. 1B). To normalize the proteins' peak areas, a SEC standard composed of five protein complexes (alcohol dehydrogenase, beta-amylase, apo-ferritin, carbonic anhydrase and thyroglobulin) was spiked into the samples before SEC and a bovine serum albumin (BSA) digest standard before LC-MS/MS analysis (Fig. 1A). Each SEC chromatogram was fractionated in 54 fractions that were individually analyzed by high-resolution nanoLC-MS/MS following the spike-in of the tryptic BSA. In total, 2 × 54 fractions for the light condition and 2 × 54 fractions for the dark condition were analyzed, leading to 216 high-resolution nanoLC-MS/MS experiments performed.

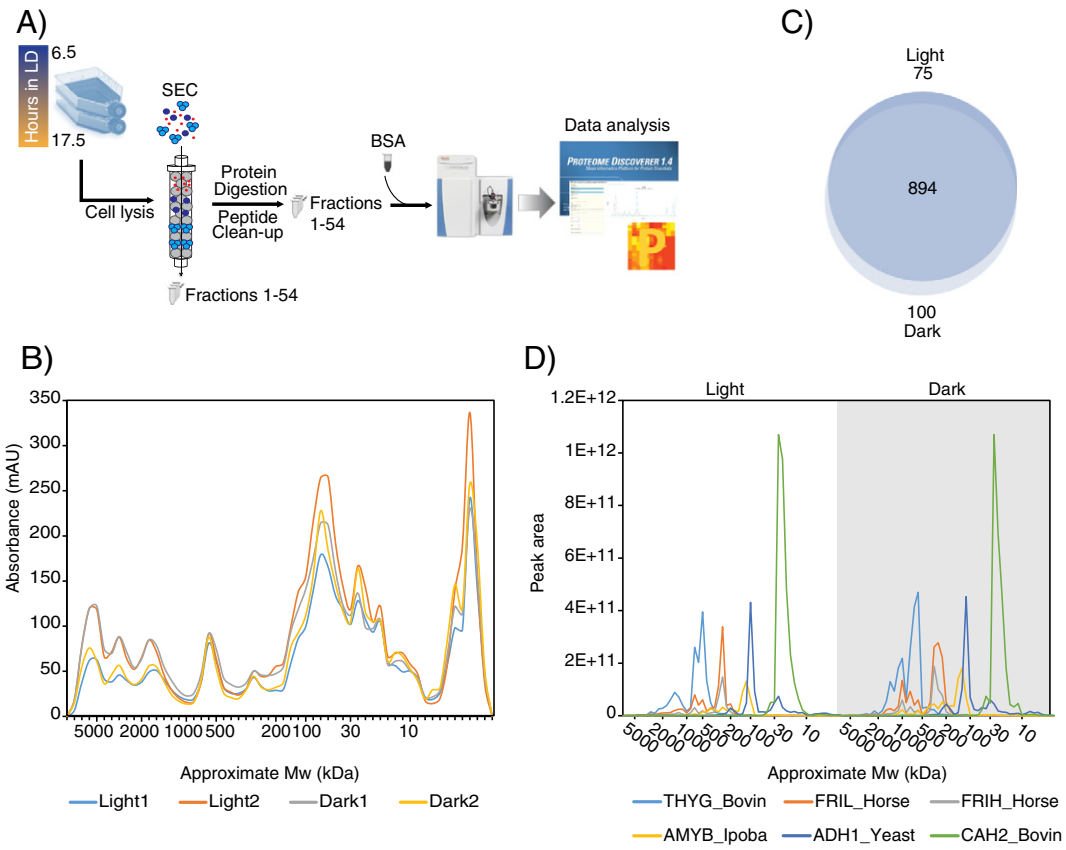

Fig. 1. Native size exclusion chromatography of *S. elongatus* protein complexes. A) *S. elongatus* cells were synchronized and cultured in LD (12:12 h) conditions. Samples were collected from two time-points separated by 12 h across a 24-h LD cycle. Mild cell lysis conditions enabled native protein complex preservation, followed by separation according to their complex/protein size using SEC. B) SEC chromatogram reproducibility across light and dark samples and corresponding replicates. C) Overlap of protein identifications between light and dark conditions. D) SEC standards elution profiles for light and dark conditions, after replicate normalization and averaging.

In the data analysis, only proteins identified with two or more peptides were considered, resulting in confident identification of 1061 proteins across the light and dark phases, with an overlap of ~84% (Fig. 1C). To measure the reproducibility, a Pearson correlation was calculated for each fraction comparing the light and dark replicates, which showed high correlation with an average of 0.8. Next, the normalized peak areas were averaged between the two replicates of each experiment, to allow quantitative comparisons, resulting in very similar peak areas of the spiked-in five SEC internal protein complex standards for the light and dark experiments (Fig. 1D), indicating correct normalization.

3.1. Global clustering analysis

To compare the SEC elution profiles of each protein in the light and in the dark phase, we performed an unsupervised hierarchical clustering analysis taking both LD profiles in parallel (Fig. 2), using Perseus software (http://www.perseus-framework.org/). Generally, similar elution profiles between the light and dark cycle were obtained, albeit that several distinct differences between the two conditions were observed. The main differences are relative abundance variation and to a lesser extent spread of the corresponding elution peaks. In some specific cases proteins were found eluting in certain SEC fractions only in either the light or dark phase, as discussed further below. Here we will focus on proteins identified eluting in the high molecular weight (Mw) range, as shown in Fig. 2, which was particularly enriched for 70S ribosome and many proteins involved in photosynthesis. This is as expected since the native molecular weight of these complexes is in the mega-(M)Da range. Also the RNA polymerase complex could be observed quite distinctively, appearing isolated in one relatively narrow SEC cluster. These complexes will be examined and described in more detail in the next sections. Of note, many other proteins were observed to elute at high Mw ranges. However, many proteins in cyanobacteria are only weakly functionally annotated and even less is known about their quaternary structure and/or contribution/association into larger protein complexes. Illustratively, ~30% of all proteins identified in our analysis are annotated as functionally uncharacterized. Our experiments may be the first evidence of their presences and/or association within larger assemblies in cyanobacteria. However, as little is known about these proteins we chose to focus on the better-annotated protein assemblies. The clusters containing the main MDa protein assemblies contained, apart from several uncharacterized proteins, also some proteins with no known interaction or related biological function. These proteins originate from upstream or downstream cellular processes in some cases, or from the same cellular localization (*e.g.* non-photosynthetic membrane proteins). We also found proteins from unrelated metabolic pathways, in some cases interacting with each other (according to the String database). Although such proteins are potential novel interactors we cannot validate this and therefore, to minimize elution biases, we performed separate cluster analysis for the MDa complexes containing the complex constituents and known or highly probable interactors (based on common biological processes).

3.2. RNA polymerase

In the global clustering analysis we observed a clear cluster enriched for the RNA polymerase (RNAP) complex (Fig. 2(a) and Suppl. Fig. 1 in the online version at http://dx.doi.org/10.1016/j.jprot.2016.04.030.), eluting around ~500 kDa. Like in *E. coli*, in cyanobacteria this complex is typically constituted of two alpha subunits, a beta and a beta′ subunit and an omega subunit, all identified in our analysis. The cyanobacterial

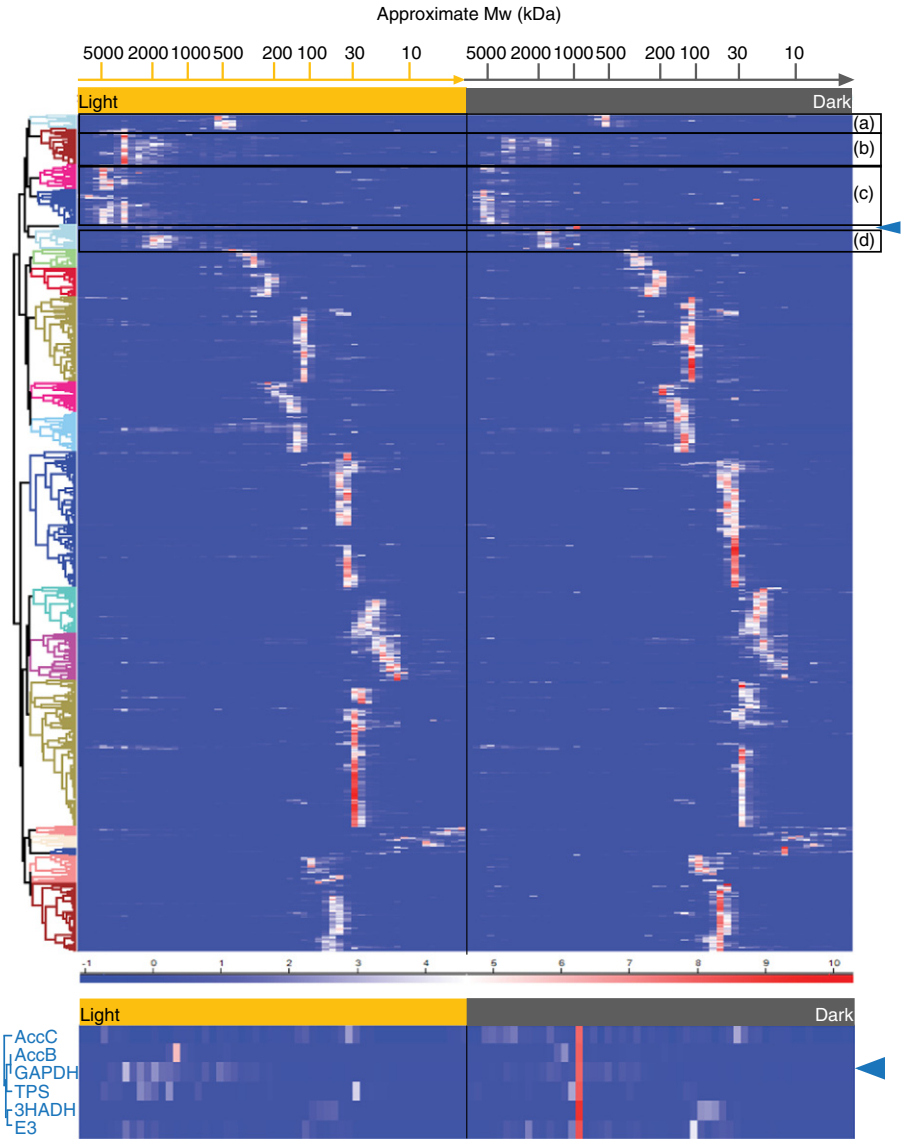

Fig. 2. Hierarchical clustering of all identified proteins. Depicted heatmap of unsupervised hierarchical clustering taking the standardized (Z-score) LD profiles in parallel, using Perseus software, as described in the methods section. Red corresponds to higher protein abundance and blue to lower abundance. Cluster enrichment in the MDa range: a) RNA polymerase; b) 50S ribosomal proteins; c) photosynthetic proteins; d) 30S ribosomal proteins; blue arrow (zoom-in below): LD dynamic cluster.

RNAP has also a gamma subunit which originates from the beta′ subunit of *E. coli* [31]. This cyanobacterial core-complex should have a theoretical Mw of ~415 kDa. For transcription, this core RNA polymerase enzyme complex recruits a variety of sigma factors enabling transcription of specific DNA template strands. If we zoom into the RNAP protein core complex profiles, we first see a substantial higher abundance of all core-components during the light phase (Fig. 3A). In our earlier cyanobacterial circadian proteome study, where we reanalyzed transcript data from Ito et al. [5], we did observe that certain components of the RNAP (alpha, beta′ and SigA1) indeed exhibit circadian rhythms in their transcripts, but not in their protein abundances [4]. Moreover, here the components of this core-complex are observed in several distinct fractions, also depending on the light or dark conditions. This likely indicates that other accessory proteins co-assemble to this complex depending on the LD phases. To investigate the nature of these possible interactors of the RNAP, a hierarchical clustering was performed only for the RNA polymerase and transcriptional related proteins (Suppl. Fig. 1 in the online version at http://dx.doi.org/10.1016/j.jprot.2016.04.030.). The targeted clustering analysis, reveals that the RNAP core complex elutes together with one of the expected sigma factors SigA1 (light and dark) and the diguanylate cyclase/phosphodiesterase with PAS/PAC and GAF sensor(S) (DGC/PDE) (only light). As described above, the sigma factor assists RNAP in binding to the correct location on the DNA – the −10 region within the promoter – for transcription initiation [32]. The phosphodiesterase is related to transcription regulation, albeit primarily through its phosphorelay sensor kinase activity. This protein was only detected in the light phase and it is known that the PAS domains are associated with monitoring of light changes [33]. Therefore, this potential co-assembly might be related to differential gene expression control.

In the targeted clustering analysis we also detected the circadian clock protein kinase KaiC (light and dark), as a transcriptional regulator. KaiC elutes across different fractions, including together with the RNAP complex, SigA1 and DGC/PDE. Since interactions between the central clock proteins, transcription factors [9] and sensor proteins [34,35] have been suggested, our data make it plausible that KaiC interacts

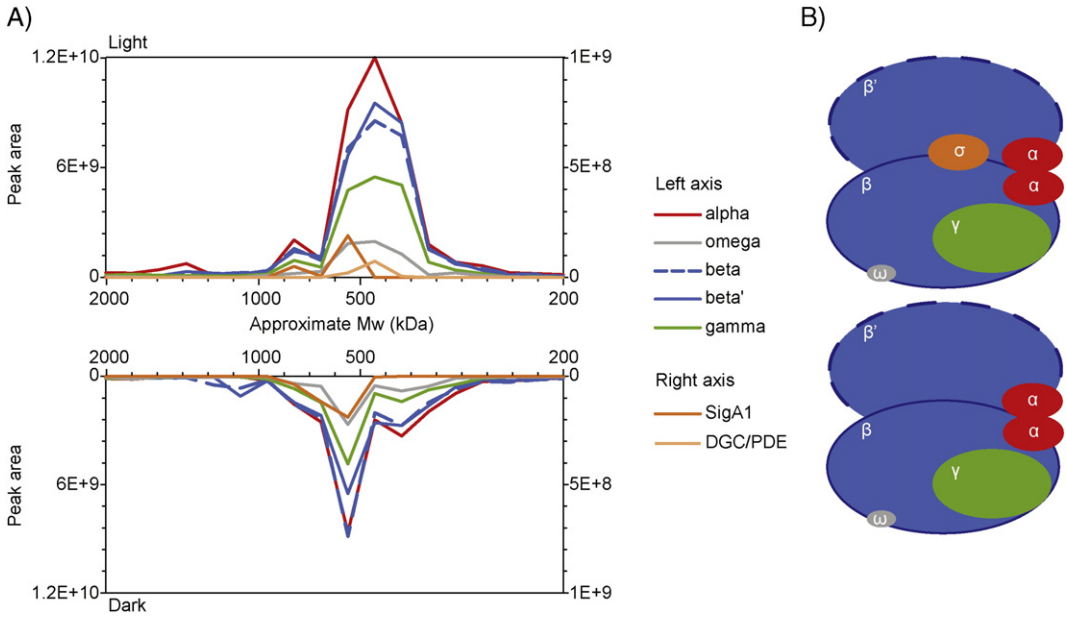

Fig. 3. RNA polymerase complex dynamics. A) SEC protein LD profiles of RNA polymerase subunits and co-eluting proteins. Essentially two types of interactions were detected; RNA polymerase with and without its sigma factor (SigA1). In the light phase RNA polymerase additionally co-elutes with the Diguanylate cyclase/Phosphodiesterase with PAS/PAC and GAF sensors (DGC/PDE). A different intensity scale is represented on the right y-axis of the plots, for amplification of the SigA1 and DGC/PDE profiles. B) Simplistic representation of both complexes.

with SigA1 and DGC/PDE. Notably, in our analysis KaiC also co-elutes at much higher Mw (~4 MDa) with several DNA binding proteins, related to DNA replication and repair.

In summary, considering the predicted Mw and the co-elution patterns, we observe the interaction of the RNAP core-complex with SigA1 and the DGC/PDE dimer, during the light phase (Fig. 3A). There is also an interaction of the RNAP complex and SigA1 with the KaiC hexamer (Suppl. Fig. 1 in the online version at http://dx.doi.org/10.1016/j.jprot.2016.04.030.). During the dark phase the RNAP core-complex can be seen alone, interacting with SigA1 (Fig. 3A–B) and with KaiC (Suppl. Fig. 1 in the online version at http://dx.doi.org/10.1016/j.jprot.2016.04.030.). Our data clearly highlight the cyclic behavior of these assemblies.

3.3. Ribosomal complex

The bacterial ribosome (70S) is composed of two subunits, the small (30S) and the large (50S). In this study, we were able to identify all proteins of the ribosomal complex, where 20 proteins from the 30S subunit and 27 from the 50S subunit passed our stringent filtering criteria. The S20 protein, from the 30S subunit, and 4 proteins from the 50S subunit (L16, L32, L34 and L36) were identified with only one unique peptide. In the global clustering analysis, most of the ribosomal proteins co-eluted, being enriched in two different clusters (Fig. 2(b) and (d)). To have a closer look at the ribosome and its potential interactors, we performed a clustering analysis on the small and large ribosomal subunits and proteins that are known to bind to the ribosome, such as those involved in the regulatory steps of translation, co-translational modifications and ribosome biogenesis (Fig. 4 and Suppl. Fig. 2 in the online version at http://dx.doi.org/10.1016/j.jprot.2016.04.030.). In the resulting heatmap, we can clearly see a separation of the small 30S subunit and the large 50S subunit. The small subunit eluted at ~1.5–2 MDa and the large subunit at ~3.5 MDa. The total molecular weight for the ribosome is 2.5 MDa, meaning that in our SEC analysis they have an apparent higher Mw. This has been observed before, where it was found that the rRNAs belonging to these subunits were not detached in the course of the analysis [26]. Potentially we capture these ribosomal complexes in different stages of maturation or even as polysomes.

Looking closer into the 50S cluster, we observe the co-elution of two initiation factors (IF-2 and IF-3) (blue arrows Fig. 4A), where IF2 is most abundant when co-eluting with the 50S subunit and IF3 with the 30S subunit. It is noticeable that IF-3 co-elutes with the peak of the 30S subunit at a higher abundance during the dark phase and in similar abundance with 50S during the light phase, which is in agreement with the translation initiation complex being initially constituted of the 30S subunit and IF-3 [36]. On the other hand, this can also indicate a dynamic relation between the initiation complex formation and the ribosome formation, the latter being more frequent during the day. If we look at the 30S cluster, we find also the RNA methyltransferase TrmH (brown arrow Fig. 4A and B, Suppl. Fig. 2 in the online version at http://dx.doi.org/10.1016/j.jprot.2016.04.030.). This methyltransferase is involved in the biogenesis of the ribosome, more specifically in the modification and maturation of the rRNA. This important factor was previously observed to have a possible interaction with the 30S particle [26].

There are other proteins co-eluting with the two main subunits, yet are not included in the same cluster due to small profile differences. These co-eluting proteins include the bacterial translation initiation factor 1 (BIF-1) and the rRNA small subunit methyltransferase A (30S Mtase A) (Fig. 4B, bottom graph). The fact that they mainly co-elute with the 30S subunit in the dark phase is causing the difference in the profiles. For now there is no obvious explanation for this observation, however it is known that the methyltransferase exerts its function in the biogenesis of the 30S particle. BIF-1, as an initiation factor, is primarily associated to the small subunit [36]. Also eluting with the ribosome, we observe the ribosome maturation factor RimP, involved in rRNA processing (Suppl. Fig. 2 in the online version at http://dx.doi.org/10.1016/j.jprot.2016.04.030.).

The DnaK/Hsp70 and GrpE (chaperone and co-chaperone) do co-elute with several ribosomal proteins, namely in the L10-L7/L12 stalk, at a lower mass (Fig. 4C and D). The same occurs for the elongation factor EF-G, EF-Ts and the sigma54 modulation protein/SSU ribosomal protein S30P (SSU S30P) (Suppl. Fig. 2 in the online version at http://dx.doi.org/10.1016/j.jprot.2016.04.030.).This is expected, as these proteins are supposed to bind to that specific ribosomal region. Moreover, it was suggested that in Eukaryotic cells L12 orthologs exist in an unbound state and L12 is part of a regulatory recruitment mechanism of

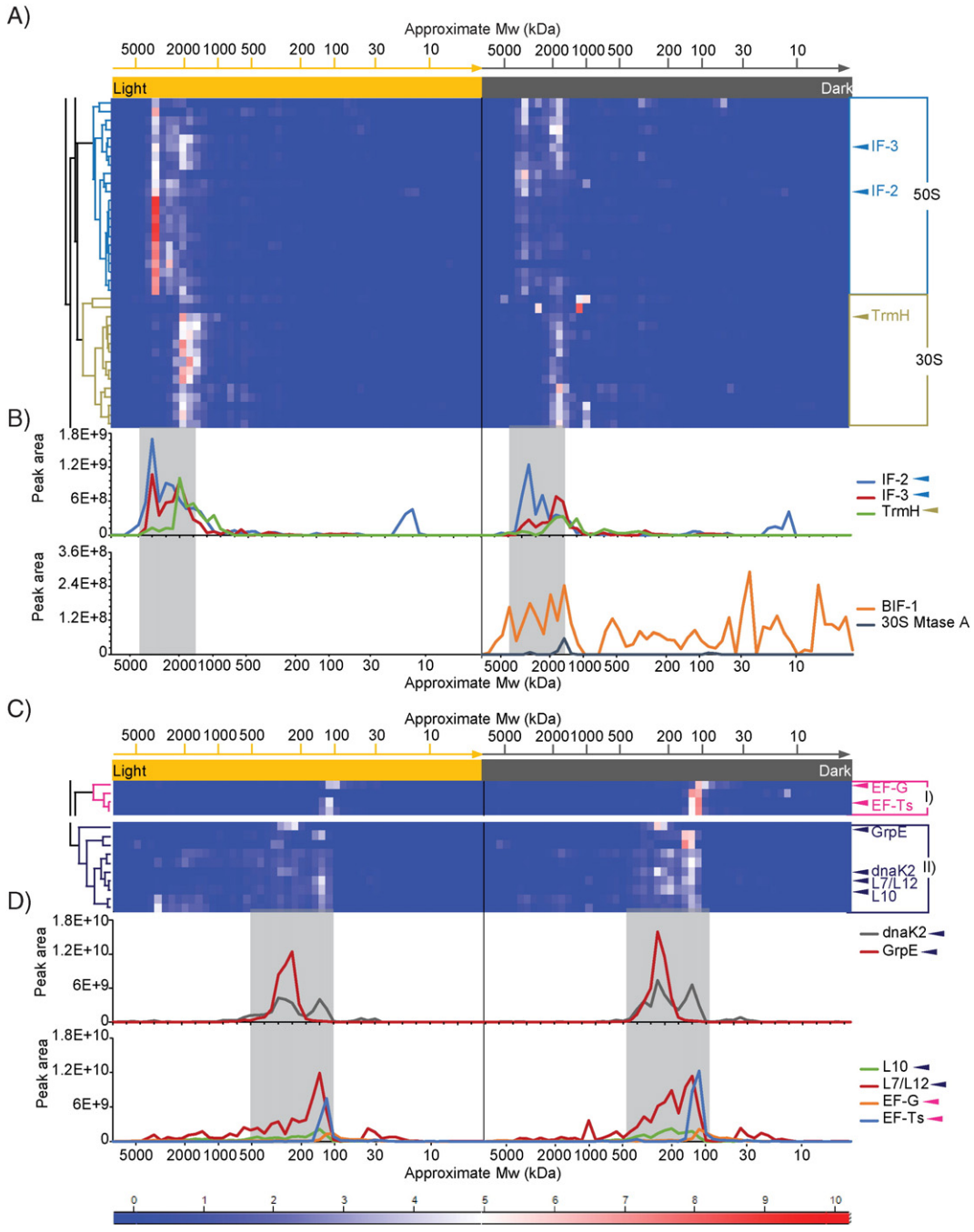

Fig. 4. Dynamic association of ribosomal and translation related proteins. Detailed heatmap of the unsupervised hierarchical clustering, performed with the standardized (Z-score) LD profiles of the ribosomal and translation related proteins in parallel, as described in the methods section. Red corresponds to higher protein abundance and blue to lower abundance. Grey areas emphasize co-elution in the profiles. A) 50S and 30S enriched clusters and protein elution profiles of co-eluting translation factors. B) L7/12 stalk cluster and co-eluting translation factors and chaperones, with individual elution profiles below for clarification purposes.

translational factors [37]. Despite the fact that in *E. coli* this was stated to be unlikely [38], our results suggest such behavior in cyanobacteria.

Comparing the light and dark conditions, we see very similar trends (Fig. 4 and Suppl. Fig. 2 in the online version at http://dx.doi.org/10.1016/j.jprot.2016.04.030.). However, in the light phase, the peak areas of the ribosomal subunits are more intense. These observations seem to show that the effective and functional ribosome or ribosomes are more prominent during the light phase, showing more dynamic interchanges between its different states. In our previous global proteomics study the ribosomal proteins showed cyclic 48 h profiles at the transcript level (re-analyzed data from Ito et al. [5]) and cyclic differences between light and dark at the proteome level [4]. The now observed pattern occurs in an opposite manner than the one obtained by global proteomics, which might be attributed to the fact that during the dark phase the majority of the proteins are in a free form and during the light phase most of the proteins form larger assemblies.

3.4. Complexes involved in photosynthesis

Another prominent set of two clusters in the global cluster analysis is enriched for the photosynthetic and thylakoid membrane-associated proteins (Fig. 2(c)). The photosynthetic pathway is essentially composed of six major complexes: phycobilisome, photosystem I (PSI) and II (PSII), cytochrome *b6f*, NAD(P)H-quinone oxireductase complex

(NDH-1) and ATP synthase. In the clustering analysis, we included the 52 proteins that we were able to identify, out of the 91 proteins that make up these complexes (Suppl. Fig. 3 in the online version at http://dx.doi.org/10.1016/j.jprot.2016.04.030.). Below, we will mainly discuss the phycobilisome, the PSI and PSII complexes.

Looking at the photosystems separately, we see that the corresponding core of each complex clusters together (Fig. 5). In the case of photosystem I (Fig. 5A), the proteins eluting at high mass include the P700 chlorophyll *a* apo-protein A1 (PsaA) and A2 (PsaB) (core complex of PSI monomer), the reaction center subunits III (PsaF) and XI (PsaL) (at the interface between PSI monomers) and the iron-sulfur center protein (PsaC) and the reaction center subunit IV (PsaE) (cytoplasm side). The NDH-1 complex co-elutes with PSI at high Mw, which agrees with their involvement in the cyclic electron flow process during photosynthesis [39]. For the photosystem II (Fig. 5B (I)), among the proteins eluting at higher mass, we observe the CP47 chlorophyll apo-protein (CP47), the 44 kDa reaction center protein (CP43) and the D2 protein (D2) (core complex of PSII monomer), the manganese-stabilizing polypeptide (PsbO) and lipoprotein Psb27 (Psb27) (luminal side). Additionally, the cytochrome *b*6-*f* complex iron-sulfur subunit (Cyt *b*6-*f*) was found to co-elute at high Mw (Suppl. Fig. 3A in the online version at http://dx.doi.org/10.1016/j.jprot.2016.04.030.). This complex is

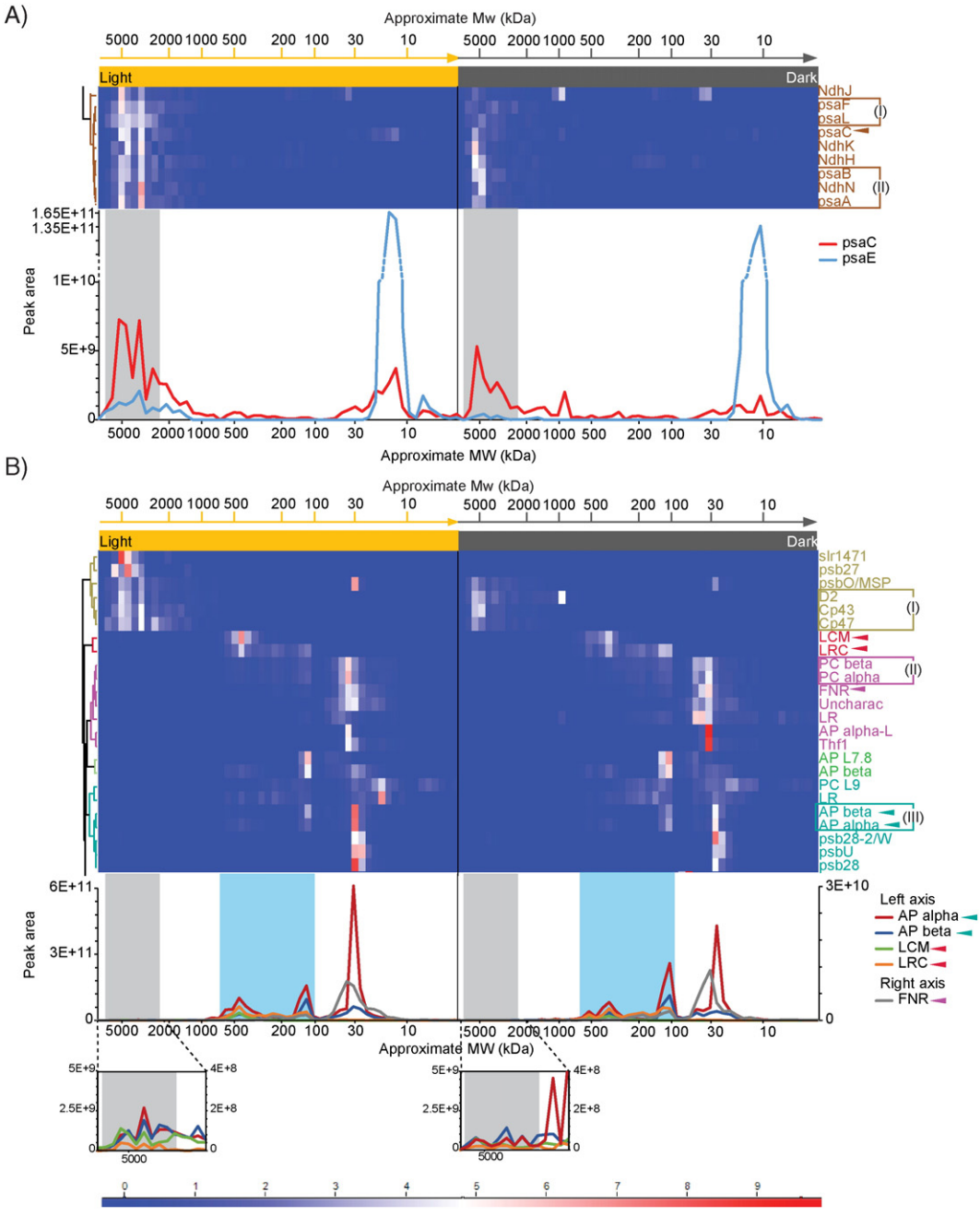

Fig. 5. Dynamics of the proteins from the photosynthetic pathway. Detailed heatmap of the unsupervised hierarchical clustering, performed with the standardized (Z-score) LD profiles of the photosynthetic proteins in parallel, as described in the methods section. Red corresponds to higher protein abundance and blue to lower abundance. Grey and blue areas emphasize co-elution in the profiles. A) Cluster of the proteins from the photosystem I (PSI) and NAD(P)H-quinoneoxireductase complexes (NDH-1); highlighted SEC LD profiles: I) Photosystem I interfaces and II) Photosystem I core (psaB and psaA). PsaE and PsaC profiles shown below demonstrate their elution at the MDa range. Dashed line indicates a break in the scale. B) Heatmap of proteins from the photosystem II (PSII) and phycobilisome complexes; highlighted SEC LD profiles: I) Photosystem II core proteins, II) Phycobilisome rod proteins, III) Phycobilisome core proteins. Profiles below demonstrate the co-elution of L_{CM}, L_{RC}, AP alpha and beta at the MDa range (zoomed in); and the co-elution of FNR (right axis) with the core proteins (AP).

responsible for electron transfer between the PSI and PSII and the cyclic electron transfer [40]. In this range, the PSII subunits elute in different fractions leading to the possibility of different states of the photosystem. It is interesting to see that, in those different states, Psb27 and PsbO do not always co-elute. This is in line with a previous report [41], which shows that these two proteins bind in the same place. During the PSII *de novo* assembly, Psb27 binds at an earlier stage than PsbO.

When comparing the light and dark conditions, the complexes show more dynamic interactions and higher intensity during the light phase. This observation can be easily explained by the photosynthetic function of these complexes during the light phase, while they are apparently actively down regulated during the dark phase. Similar to the observations made for the ribosome data, most proteins belonging to the phycobilisome system displayed a cyclic pattern between light and dark in our previous global proteomics study [4], but in an opposite manner, being higher during the night phase. An explanation similar to the ribosomal complex can be applied, in which protein complexes are disassembled during the night and proteins are more abundantly present as single entities.

The main proteins of both PSI and PSII, namely the core proteins, the luminal side from PSI and the interfaces from PSI, co-eluted in the high mass range. They do not interact physically, but they are usually found in close proximity, in order to ensure the electron flow. The fact that they elute together at such high Mw (4 MDa) could be explained by an indirect interaction between the PSI and PSII, through the ferredoxin-$NADP^+$ oxidoreductase (FNR) and the phycobilisome (discussed below), which was suggested before [42,43].

Next, we looked more specifically at the phycobilisome complex (Fig. 5B). The phycobilisome acts as an antenna, harvesting the photon-energy. It is composed of a core complex with allophycocyanins (AP) and its linkers; and several rod complexes with phycocyanins (PC) and its linkers. We were able to identify all of its components as well as their assembly factors (Suppl. Fig. 3 in the online version at http://dx.doi.org/10.1016/j.jprot.2016.04.030.). In the heatmap in Fig. 5B, we can see a clear differentiation between these sub-complexes, namely the rod (II) and core (III) proteins. We also noticed specific interactions within these sub-complexes. In the rod complex, we see a clear co-elution with FNR which is associated with PSI (Fig. 5B, light blue area). FNR is in turn also eluting at high Mw with a lower abundance. This coincides with our previous observation for an interaction of PSI with PSII, which could have a very transient nature and is mediated by the interaction of FNR with the phycobilisome complex and PSI, and the interaction of the phycobilisome with PSII. Additionally, we see the core-membrane linker (L_{CM}) eluting in the 4 MDa range (Fig. 5B, zoom in), demonstrating the interaction of phycobilisome and PSI further. This is in line with the recent identification of a megacomplex (MCL), consisting of phycobilisome-PSII-PSI, with L_{CM} as the central binding place for PSI [44]. The L_{CM} itself is more prominent in light conditions and mostly at high mass, co-eluting with the AP alpha, AP beta and the rod-core linker (L_{RC}), which stabilizes the connection between the rods and the core, facilitating energy transfer (Fig. 5B, grey and blue areas); but also with PSII proteins, which are the ultimate energy receivers (Fig. 5B, heatmap). These interactions indicate an active antenna complex (phycobilisome-PSII-PSI) during the light phase. The rest of the linkers located in the rod and core structures, have a more variable distribution across the fractions. Since we also observe greater variability of Mw within the rod proteins, we can speculate that these are related to the dynamic characteristics of the rods, which have been shown to vary in number of single units according to the light changes [42].

3.5. Light versus dark dynamics

Our global clustering analysis revealed several dynamic protein complex elution profiles. One case of extreme difference between the light and dark phase concerns a group of proteins that do not co-elute during the light phase, but during the dark phase align around one MDa (Fig. 2 blue arrow and Fig. 6A). In this cluster, we find 3-hydroxyacid dehydrogenase (3HADH), dihydroplipoyl dehydrogenase (E3), thiamine-phosphate synthase (TPS), acetyl-coenzyme A (acetyl-CoA) carboxylase carboxyltransferase subunit alpha/biotin carboxylase (AccC), biotin carboxyl carrier protein (AccB) and glyceraldehyde-3-phosphate dehydrogenase (GAPDH). An immediate connection between these proteins is not easily made, since in the search tool commonly used for the retrieval of interacting genes/proteins (STRING) [45], the only known interaction with medium confidence is the one between AccB and AccC. These two proteins are part of the acetyl-CoA carboxylase complex hexamer (ACC), from which we also were able to identify the subunit AccD. If we look closer into these proteins' profiles (Fig. 6B), we see that the AccB elutes alone in the light phase, but it elutes together with AccC in the dark phase. However, the interaction between these two does not make up for the total mass corresponding to the fraction where they elute, unless they oligomerize (~1 MDa). If we look at other proteins in this cluster we can make similar observations. For the GAPDH, we could identify known interactors in our dataset: the phosphoribulokinase (Prk) and the linker CP12 [46–48]. Prk and GAPDH are key enzymes in carbon fixation, through the Calvin cycle, which occurs within the light phase. As expected, the GAPDH-CP12-Prk complex co-elutes more prominently in the dark phase, since their association at night corresponds to their inactive state (Fig. 6C). In the case of the E3 protein, which is part of different multi-enzyme α-keto acid dehydrogenases, we were also able to find known interactors, which make up the pyruvate dehydrogenase (PDC): the pyruvate dehydrogenase E1 component subunit alpha (E1α), the pyruvate/2-oxoglutarate dehydrogenase complex dehydrogenase (E1β) component (beta subunit) and the pyruvate dehydrogenase dihydrolipoamide acetyltransferase component (E2) [49,50]. These proteins form a complex of ~4 MDa, which is visible in the SEC profile (Fig. 6D). This megadalton PDC appears to exist mainly during the light phase. However, during the dark phase, only the E3 component elutes at 1 MDa, aligning with the rest of the cluster in fig. 6A. By extending the STRING network to all these different components observed eluting at 1 MDa, we now find a possible interaction between the PDC and the ACC (Fig. 6E). The PDC is involved in the formation of Acetyl-CoA from pyruvate, which leads to synthesis of citric acid, in the citric acid cycle. ACC on the other hand is activated by citric acid and uses acetyl-CoA in fatty acid metabolism. These common aspects can culminate in an effective interaction related to their regulation.

4. Conclusion

In summary, we report the first global analysis of macromolecular assemblies in the cyanobacterium *S. elongatus* across day (light) and night (dark) conditions. Our SEC and MS based proteomics approach enabled the identification of megadalton protein assemblies in cyanobacteria, including the ribosomal and the photosynthetic complexes. This approach, which was implemented with higher separation resolution than the previous study in chloroplasts [26], allowed us the use of hierarchical clustering of the SEC protein elution profiles to better infer particular PPIs. This methodology allowed us to infer dynamic interactions for several protein complexes such as for the sigma factor SigA1 and the phosphodiesterase sensor in the RNA polymerase complex. For the megadalton complexes, involved in transcription and photosynthesis, we observe an intensity decrease during the dark period, which is expected especially for the photosynthetic pathway. These complexes also seem to have more assembly variety during the light phase. We also observe an unexpected association of (members of) complexes that are involved in glycolysis, pyruvate metabolism and carbon fixation, which specifically cluster together in the dark phase, hinting at a common role or regulation. The differences observed between the light and dark conditions in these complexes indicate a cyclic regulation of essential cellular processes, which have been connected to circadian rhythm

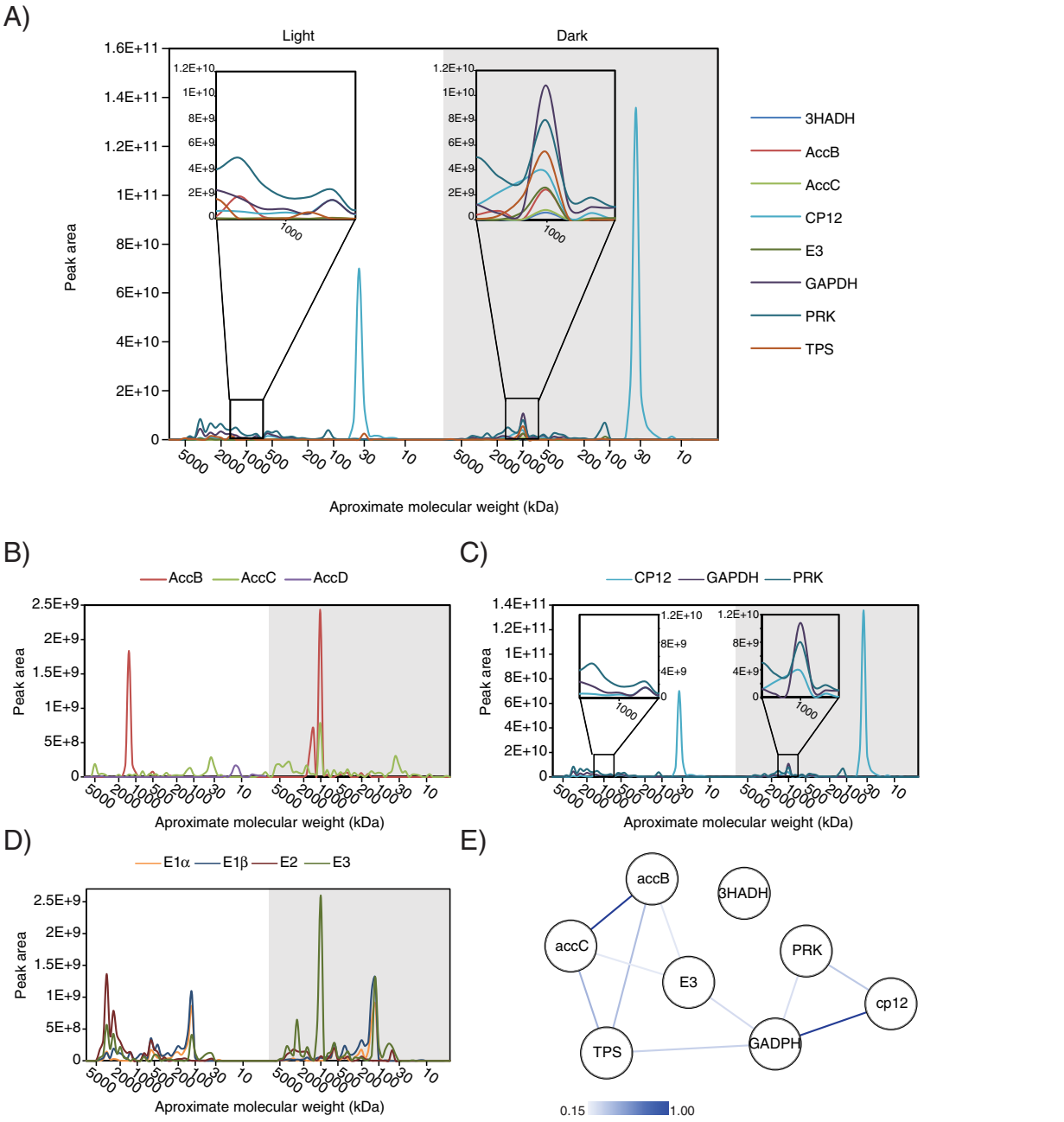

Fig. 6. Cluster with LD dynamics. A) SEC LD profiles of proteins co-eluting at 1 MDa, in dark conditions, namely 3-hidroxyacid dehydrogenase (3HADH), dihydroplipoyl dehydrogenase (E3), thiamine-phosphate synthase (TPS), acetyl-coenzyme A carboxylase carboxyl transferase subunit alpha/biotin carboxylase (AccC), biotin carboxyl carrier protein (AccB), glyceraldehyde-3-phosphate dehydrogenase (GAPDH), phosphoribulokinase (Prk) and the linker CP12. A zoom in of the 1 MDa range is shown for clarity. B) SEC LD profiles of the acetyl-CoA carboxylase complex proteins identified (AccB, AccC, AccD). C) SEC LD profiles of the carbon fixation complex GAPDH, Prk and CP12. A zoom in of the 1 MDa range is shown for clarity. D) SEC LD profiles of the pyruvate dehydrogenase complex proteins (E1α, E1β, E2, E3). E) Interaction network of the proteins co-eluting at the 1 MDa range. Interactions based on gene neighborhood, co-occurrence, co-expression, experimental evidence of interaction, pathway interaction and text mining, retrieved from STRING [45] and analyzed with Cytoscape [54].

regulation before [51–53]. In conclusion, our work demonstrates the advantages of using SEC coupled to high resolution LC-MS/MS based proteomics in the study of PPI dynamics and provides novel insights in PPIs, opening opportunities to new investigations at a more targeted level.

Supplementary data to this article can be found online at http://dx.doi.org/10.1016/j.jprot.2016.04.030.

Transparency document

The Transparency document associated with this article can be found, in online version.

Acknowledgements

This work was partly supported by the PRIME-XS project (grant agreement number 262067) funded by the European Union 7th Framework Program. This work is part of the project Proteins At Work, a program of the Netherlands Proteomics Centre financed by the Netherlands Organization for Scientific Research (NWO) as part of the National Roadmap Large-scale Research Facilities of the Netherlands (project number 184.032.201). A.F.M.A. acknowledges additional support by the Netherlands Organization for Scientific Research (NWO) through a VIDI grant (723.012.102).

References

[1] C.H. Johnson, P.L. Stewart, M. Egli, The cyanobacterial circadian system: from biophysics to bioevolution, Annu. Rev. Biophys. 40 (2011) 143–167, http://dx.doi.org/10.1146/annurev-biophys-042910-155317.

[2] C.K. Holtman, Y. Chen, P. Sandoval, A. Gonzales, M.S. Nalty, T.L. Thomas, et al., High-throughput functional analysis of the *Synechococcus elongatus* PCC 7942 genome, DNA Res. 12 (2005) 103–115, http://dx.doi.org/10.1093/dnares/12.2.103.

[3] C.R. Andersson, N.F. Tsinoremas, J. Shelton, N.V. Lebedeva, J. Yarrow, H. Min, et al., ScienceDirect.com - methods in enzymology - application of bioluminescence to the study of circadian rhythms in cyanobacteria, Methods Enzymol. 305 (2000) 527–542https://www.sciencedirect.com/science/article/pii/S0076687900055117.

[4] A.C.L. Guerreiro, M. Benevento, R. Lehmann, B. van Breukelen, H. Post, P. Giansanti, et al., Daily rhythms in the cyanobacterium *Synechococcus elongatus* probed by high-resolution mass spectrometry-based proteomics reveals a small defined set of cyclic proteins, Mol. Cell. Proteomics 13 (2014) 2042–2055, http://dx.doi.org/10.1074/mcp.M113.035840.

[5] H. Ito, M. Mutsuda, Y. Murayama, J. Tomita, N. Hosokawa, K. Terauchi, et al., Cyanobacterial daily life with Kai-based circadian and diurnal genome-wide transcriptional control in *Synechococcus elongatus*, Proc. Natl. Acad. Sci. U. S. A. 106 (2009) 14168–14173, http://dx.doi.org/10.1073/pnas.0902587106.

[6] C. Brettschneider, R.J. Rose, S. Hertel, I.M. Axmann, A.J.R. Heck, M. Kollmann, A sequestration feedback determines dynamics and temperature entrainment of the KaiABC circadian clock, Mol. Syst. Biol. 6 (2010) 389, http://dx.doi.org/10.1038/msb.2010.44.

[7] M. Nakajima, K. Imai, H. Ito, T. Nishiwaki, Y. Murayama, H. Iwasaki, et al., Reconstitution of circadian oscillation of cyanobacterial KaiC phosphorylation in vitro, Science 308 (2005) 414–415, http://dx.doi.org/10.1126/science.1108451.

[8] V. Vijayan, I.H. Jain, E.K. O'Shea, A high resolution map of a cyanobacterial transcriptome, Genome Biol. 12 (2011) R47, http://dx.doi.org/10.1186/gb-2011-12-5-r47.

[9] N. Takai, M. Nakajima, T. Oyama, R. Kito, C. Sugita, M. Sugita, et al., A KaiC-associating SasA-RpaA two-component regulatory system as a major circadian timing mediator in cyanobacteria, Proc. Natl. Acad. Sci. U. S. A. 103 (2006), 12109–14http://dx.doi.org/10.1073/pnas.0602955103.

[10] H. Iwasaki, S.B. Williams, Y. Kitayama, M. Ishiura, S.S. Golden, T. Kondo, A KaiC-interacting sensory histidine kinase, SasA, necessary to sustain robust circadian oscillation in cyanobacteria, Cell 101 (2000) 223–233 https://www.sciencedirect.com/science/article/pii/S0092867400808326 (accessed February 22, 2013).

[11] J.S. Markson, J.R. Piechura, A.M. Puszynska, E.K. O'Shea, Circadian control of global gene expression by the cyanobacterial master regulator RpaA, Cell 155 (2013) 1396–1408, http://dx.doi.org/10.1016/j.cell.2013.11.005.

[12] M. Hanaoka, N. Takai, N. Hosokawa, M. Fujiwara, Y. Akimoto, N. Kobori, et al., RpaB, another response regulator operating circadian clock-dependent transcriptional regulation in *Synechococcus elongatus* PCC 7942, J. Biol. Chem. 287 (2012) 26321–26327, http://dx.doi.org/10.1074/jbc.M111.338251.

[13] Y. Taniguchi, N. Takai, M. Katayama, T. Kondo, T. Oyama, Three major output pathways from the KaiABC-based oscillator cooperate to generate robust circadian kaiBC expression in cyanobacteria, Proc. Natl. Acad. Sci. U. S. A. 107 (2010) 3263–3268, http://dx.doi.org/10.1073/pnas.0909924107.

[14] O. Schmitz, CikA, a bacteriophytochrome that resets the cyanobacterial circadian clock, Science 289 (80-.) (2000) 765–768, http://dx.doi.org/10.1126/science.289.5480.765.

[15] S.R. Mackey, J.-S. Choi, Y. Kitayama, H. Iwasaki, G. Dong, S.S. Golden, Proteins found in a CikA interaction assay link the circadian clock, metabolism, and cell division in *Synechococcus elongatus*, J. Bacteriol. 190 (2008) 3738–3746, http://dx.doi.org/10.1128/JB.01721-07.

[16] T. Rolland, M. Taşan, B. Charloteaux, S.J. Pevzner, Q. Zhong, N. Sahni, et al., A proteome-scale map of the human interactome network, Cell 159 (2014) 1212–1226, http://dx.doi.org/10.1016/j.cell.2014.10.050.

[17] W.H. Dunham, M. Mullin, A.-C. Gingras, Affinity-purification coupled to mass spectrometry: basic principles and strategies, Proteomics 12 (2012) 1576–1590, http://dx.doi.org/10.1002/pmic.201100523.

[18] A.F.M. Altelaar, J. Munoz, A.J.R. Heck, Next-generation proteomics: towards an integrative view of proteome dynamics, Nat. Rev. Genet. 14 (2013) 35–48, http://dx.doi.org/10.1038/nrg3356.

[19] M.O. Collins, J.S. Choudhary, Mapping multiprotein complexes by affinity purification and mass spectrometry, Curr. Opin. Biotechnol. 19 (2008) 324–330, http://dx.doi.org/10.1016/j.copbio.2008.06.002.

[20] A.-C. Gingras, M. Gstaiger, B. Raught, R. Aebersold, Analysis of protein complexes using mass spectrometry, Nat. Rev. Mol. Cell Biol. 8 (2007) 645–654, http://dx.doi.org/10.1038/nrm2208.

[21] N.A. Binai, F. Marino, P. Soendergaard, N. Bache, S. Mohammed, A.J.R. Heck, Rapid analyses of proteomes and interactomes using an integrated solid-phase extraction-liquid chromatography-MS/MS system, J. Proteome Res. 14 (2015) 977–985, http://dx.doi.org/10.1021/pr501011z.

[22] F. Hosp, R.A. Scheltema, C. Eberl, N.A. Kulak, E.C. Keilhauer, K. Mayr, et al., A double-barrel LC-MS/MS system to quantify 96 interactomes per day, Mol. Cell. Proteomics (2015)http://dx.doi.org/10.1074/mcp.O115.049460.

[23] G. Butland, J.M. Peregrín-Alvarez, J. Li, W. Yang, X. Yang, V. Canadien, et al., Interaction network containing conserved and essential protein complexes in *Escherichia coli*, Nature 433 (2005) 531–537, http://dx.doi.org/10.1038/nature03239.

[24] A. Goel, D. Colcher, J.S. Koo, B.J. Booth, G. Pavlinkova, S.K. Batra, Relative position of the hexahistidine tag effects binding properties of a tumor-associated single-chain Fv construct, Biochim. Biophys. Acta 1523 (2000) 13–20 (http://www.ncbi.nlm.nih.gov/pubmed/11099853 (accessed February 17, 2015).

[25] M. Rumlová, J. Beneďiková, R. Cubínková, I. Pichová, T. Ruml, Comparison of classical and affinity purification techniques of Mason-Pfizer monkey virus capsid protein: the alteration of the product by an affinity tag, Protein Expr. Purif. 23 (2001) 75–83, http://dx.doi.org/10.1006/prep.2001.1488.

[26] P.D.B. Olinares, L. Ponnala, K.J. van Wijk, Megadalton complexes in the chloroplast stroma of *Arabidopsis thaliana* characterized by size exclusion chromatography, mass spectrometry, and hierarchical clustering, Mol. Cell. Proteomics 9 (2010) 1594–1615, http://dx.doi.org/10.1074/mcp.M000038-MCP201.

[27] A.R. Kristensen, J. Gsponer, L.J. Foster, A high-throughput approach for measuring temporal changes in the interactome, Nat. Methods 9 (2012) 907–909, http://dx.doi.org/10.1038/nmeth.2131.

[28] K.J. Kirkwood, Y. Ahmad, M. Larance, A.I. Lamond, Characterization of native protein complexes and protein isoform variation using size-fractionation-based quantitative proteomics, Mol. Cell. Proteomics 12 (2013) 3851–3873, http://dx.doi.org/10.1074/mcp.M113.032367.

[29] R. Rippka, J. Deruelles, J. Waterbury, M. Herdman, R. Stanier, Generic assignments, strain histories and properties of pure cultures of cyanobacteria, J. Gen. Microbiol. 110 (1979) 1–61 http://mic.sgmjournals.org/content/111/1/1.short (accessed October 23, 2013).

[30] J.C. Silva, M.V. Gorenstein, G.-Z. Li, J.P.C. Vissers, S.J. Geromanos, Absolute quantification of proteins by LCMSE: a virtue of parallel MS acquisition, Mol. Cell. Proteomics 5 (2006) 144–156, http://dx.doi.org/10.1074/mcp.M500230-MCP200.

[31] L. Gunnelius, K. Hakkila, J. Kurkela, H. Wada, E. Tyystjärvi, T. Tyystjärvi, The omega subunit of the RNA polymerase core directs transcription efficiency in cyanobacteria, Nucleic Acids Res. 42 (2014) 4606–4614, http://dx.doi.org/10.1093/nar/gku084.

[32] D.J. Lee, S.D. Minchin, S.J.W. Busby, Activating transcription in bacteria, Annu. Rev. Microbiol. 66 (2012) 125–152, http://dx.doi.org/10.1146/annurev-micro-092611-150012.

[33] B.L. Taylor, I.B. Zhulin, PAS domains: internal sensors of oxygen, redox potential, and light, Microbiol. Mol. Biol. Rev. 63 (1999) 479–506 http://mmbr.asm.org/content/63/2/479.full (accessed January 30, 2015).

[34] N.B. Ivleva, M.R. Bramlett, P.A. Lindahl, S.S. Golden, LdpA: a component of the circadian clock senses redox state of the cell, EMBO J. 24 (2005), 1202–10http://dx.doi.org/10.1038/sj.emboj.7600606.

[35] N.B. Ivleva, T. Gao, A.C. LiWang, S.S. Golden, Quinone sensing by the circadian input kinase of the cyanobacterial circadian clock, Proc. Natl. Acad. Sci. U. S. A. 103 (2006) 17468–17473, http://dx.doi.org/10.1073/pnas.0606639103.

[36] T.M. Schmeing, V. Ramakrishnan, What recent ribosome structures have revealed about the mechanism of translation, Nature 461 (2009) 1234–1242, http://dx.doi.org/10.1038/nature08403.

[37] P. Gonzalo, J.-P. Reboud, The puzzling lateral flexible stalk of the ribosome, Biol. Cell. 95 (2003) 179–193, http://dx.doi.org/10.1016/S0248-4900(03)00034-0.

[38] M. Diaconu, U. Kothe, F. Schlünzen, N. Fischer, J.M. Harms, A.G. Tonevitsky, et al., Structural basis for the function of the ribosomal L7/12 stalk in factor binding and GTPase activation, Cell 121 (2005) 991–1004, http://dx.doi.org/10.1016/j.cell.2005.04.015.

[39] N. Battchikova, E.-M. Aro, Cyanobacterial NDH-1 complexes: multiplicity in function and subunit composition, Physiol. Plant. 131 (2007) 22–32, http://dx.doi.org/10.1111/j.1399-3054.2007.00929.x.

[40] W.A. Cramer, H. Zhang, J. Yan, G. Kurisu, J.L. Smith, Transmembrane traffic in the cytochrome *b6f* complex, Annu. Rev. Biochem. 75 (2006) 769–790, http://dx.doi.org/10.1146/annurev.biochem.75.103004.142756.

[41] J. Nickelsen, B. Rengstl, Photosystem II assembly: from cyanobacteria to plants, Annu. Rev. Plant Biol. 64 (2013) 609–635, http://dx.doi.org/10.1146/annurev-arplant-050312-120124.

[42] R. MacColl, Cyanobacterial phycobilisomes, J. Struct. Biol. 124 (1998) 311–334, http://dx.doi.org/10.1006/jsbi.1998.4062.

[43] W.M. Schluchter, D.A. Bryant, Molecular characterization of ferredoxin-NADP$^+$ oxidoreductase in cyanobacteria: cloning and sequence of the petH gene of Synechococcus sp. PCC 7002 and studies on the gene product, Biochemistry 31 (1992) 3092–3102 (http://www.ncbi.nlm.nih.gov/pubmed/1554697 (accessed February 12, 2015).

[44] H. Liu, H. Zhang, D.M. Niedzwiedzki, M. Prado, G. He, M.L. Gross, et al., Phycobilisomes supply excitations to both photosystems in a megacomplex in cyanobacteria, Science 342 (2013) 1104–1107, http://dx.doi.org/10.1126/science.1242321.

[45] A. Franceschini, D. Szklarczyk, S. Frankild, M. Kuhn, M. Simonovic, A. Roth, et al., STRING v9.1: protein-protein interaction networks, with increased coverage and integration, Nucleic Acids Res. 41 (2013), D808–15http://dx.doi.org/10.1093/nar/gks1094.

[46] B. Gontero, L. Avilan, Creating order out of disorder: structural imprint of GAPDH on CP12, Structure 19 (2011) 1728–1729, http://dx.doi.org/10.1016/j.str.2011.11.004.

[47] T. Kitatani, Y. Nakamura, K. Wada, T. Kinoshita, M. Tamoi, S. Shigeoka, et al., Structure of apo-glyceraldehyde-3-phosphate dehydrogenase from Synechococcus PCC7942, Acta Crystallogr. Sect. F: Struct. Biol. Cryst. Commun. 62 (2006) 727–730, http://dx.doi.org/10.1107/S1744309106027916.

[48] H. Matsumura, A. Kai, T. Maeda, M. Tamoi, A. Satoh, H. Tamura, et al., Structure basis for the regulation of glyceraldehyde-3-phosphate dehydrogenase activity via the intrinsically disordered protein CP12, Structure 19 (2011) 1846–1854, http://dx.doi.org/10.1016/j.str.2011.08.016.

[49] U. Neveling, S. Bringer-Meyer, H. Sahm, Gene and subunit organization of bacterial pyruvate dehydrogenase complexes, Biochim. Biophys. Acta Protein Struct. Mol. Enzymol. 1385 (1998) 367–372, http://dx.doi.org/10.1016/S0167-4838(98)00080-6.

[50] A. Engels, U. Kahmann, H.G. Ruppel, E.K. Pistorius, Isolation, partial characterization and localization of a dihydrolipoamide dehydrogenase from the cyanobacterium Synechocystis PCC 6803, Biochim. Biophys. Acta Protein Struct. Mol. Enzymol. 1340 (1997) 33–44, http://dx.doi.org/10.1016/S0167-4838(97)00025-3.

[51] C.H. Johnson, M. Egli, Metabolic compensation and circadian resilience in prokaryotic cyanobacteria, Annu. Rev. Biochem. 83 (2014) 221–247, http://dx.doi.org/10.1146/annurev-biochem-060713-035632.
[52] X. Qin, M. Byrne, Y. Xu, T. Mori, C.H. Johnson, Coupling of a core post-translational pacemaker to a slave transcription/translation feedback loop in a circadian system, PLoS Biol. 8 (2010), e1000394http://dx.doi.org/10.1371/journal.pbio.1000394.
[53] G. Pattanayak, M.J. Rust, The cyanobacterial clock and metabolism, Curr. Opin. Microbiol. 18 (2014) 90–95, http://dx.doi.org/10.1016/j.mib.2014.02.010.
[54] P. Shannon, A. Markiel, O. Ozier, N.S. Baliga, J.T. Wang, D. Ramage, et al., Cytoscape: a software environment for integrated models of biomolecular interaction networks, Genome Res. 13 (2003) 2498–2504, http://dx.doi.org/10.1101/gr.1239303.